

See discussions, stats, and author profiles for this publication at: <https://www.researchgate.net/publication/236452668>

Isotopic composition of a calcite-cemented layer in the Lower Jurassic Bridport Sands, southern England: Implications for formation of laterally extensive calcite-cemented layers

Article in *Journal Of Sedimentary Research* · July 1993

DOI: 10.1306/D4267BB3-2B26-11D7-8648000102C1865D

CITATIONS

28

READS

79

2 authors, including:



[Olav Walderhaug](#)

Equinor

68 PUBLICATIONS 2,942 CITATIONS

[SEE PROFILE](#)

ISOTOPIC COMPOSITION OF A CALCITE-CEMENTED LAYER IN THE LOWER JURASSIC BRIDPORT SANDS, SOUTHERN ENGLAND: IMPLICATIONS FOR FORMATION OF Laterally Extensive Calcite-Cemented Layers

PER ARNE BJØRKUM¹ AND OLAV WALDERHAUG²

¹ Statoil, P.O. Box 300, N-4001 Stavanger, Norway

² Rogaland Research, P.O. Box 2503 Ullandhaug, N-4004 Stavanger, Norway

ABSTRACT: $\delta^{18}\text{O}_{\text{PDB}}$ and $\delta^{13}\text{C}_{\text{PDB}}$ values have been measured on 107 calcite cement samples from a laterally extensive (> 3 km) and continuous calcite-cemented layer 0.5 m thick in the coastal exposures of the Lower Jurassic shallow-marine Bridport Sands in Dorset, southern England. The samples were taken from a two-dimensional grid with 10-cm horizontal and vertical spacing between samples and along individual vertical lines across the calcite-cemented layer. $\delta^{18}\text{O}_{\text{PDB}}$ values vary between -4.8‰ and -9.2‰ and decrease radially outwards from points with lateral spacings on the order of 0.5–1 m in the middle of the calcite-cemented layer. The $\delta^{18}\text{O}_{\text{PDB}}$ values therefore indicate that the calcite-cemented layer was formed by merging of concretions. All $\delta^{13}\text{C}_{\text{PDB}}$ values measured are in the narrow range -2.2‰ to -0.5‰ , which suggests that the dominant source of calcite cement in the layer was biogenic carbonate.

INTRODUCTION

Several authors have suggested that calcite-cemented layers in sandstones may form by merging of concretions (Berner 1980; Fürsich 1982; Bryant et al. 1988; Walderhaug et al. 1989; Bjørkum and Walderhaug 1990). If this hypothesis is correct, a systematic spatial variation of $\delta^{18}\text{O}$ values of calcite cement in a calcite-cemented layer would be expected. Assuming that no major shifts in oxygen isotopic composition of the pore water took place during calcite precipitation and that burial depth and temperature increased with time, original nucleation points (i.e., concretion centers) should have the least negative $\delta^{18}\text{O}$ values, and the latest precipitated infill of calcite cement between the locations of original concretions should have the most negative $\delta^{18}\text{O}$ values.

Although several authors have presented $\delta^{18}\text{O}$ values of calcite cement measured at closely spaced locations across concretions in shales (Coleman and Raiswell 1981; Coniglio and Cameron 1990; Morad and Eshete 1990; Scotchman 1991), relatively little data have been published on the detailed $\delta^{18}\text{O}$ composition of calcite-cemented concretions in sandstones (Wilkinson 1991). Moreover, the published data on calcite-cemented layers in sandstones are one-dimensional, because analyses have been made along vertical lines across the calcite-cemented layers (Kantorowicz et al. 1987; Walderhaug et al. 1989); closely spaced analyses along a two-dimensional grid have, as far as we know, not been published.

In this study $\delta^{18}\text{O}_{\text{PDB}}$ and $\delta^{13}\text{C}_{\text{PDB}}$ values for calcite cement were made in a two-dimensional vertical grid located within a laterally extensive (> 3 km) calcite-cemented layer in the Lower Jurassic Bridport Sands, southern England, in order to determine whether the isotopic data indicate that the layer formed by merging of concretions.

THE BRIDPORT SANDS

The calcite-cemented layer sampled is located in the coastal exposures of the approximately 40 m thick Toarcian Bridport Sands (Wilson et al. 1958; Davies 1967, 1969; Melville and Freshney 1982; Bryant et al. 1988) south of Burton Bradstock in Dorset (Fig. 1). There, the Bridport Sands consist of bioturbated very fine lower-shoreface sandstone containing abundant calcite-cemented layers that are either continuously cemented or consist of stratabound concretions (Davies 1967; Kantorowicz et al.

1987; Bryant et al. 1988; Walderhaug et al. 1989). The calcite-cemented layers make up 20–25% of the thickness of the formation, are up to 75 cm thick, and are separated from each other by layers of friable noncemented sandstone 0.2–3 m thick. The Bridport Sands south of Burton Bradstock conformably overlie the alternating thin marine mudstone and limestone strata of the Toarcian Down Cliff Clay and are overlain by the limestones of the Bajocian Inferior Oolite.

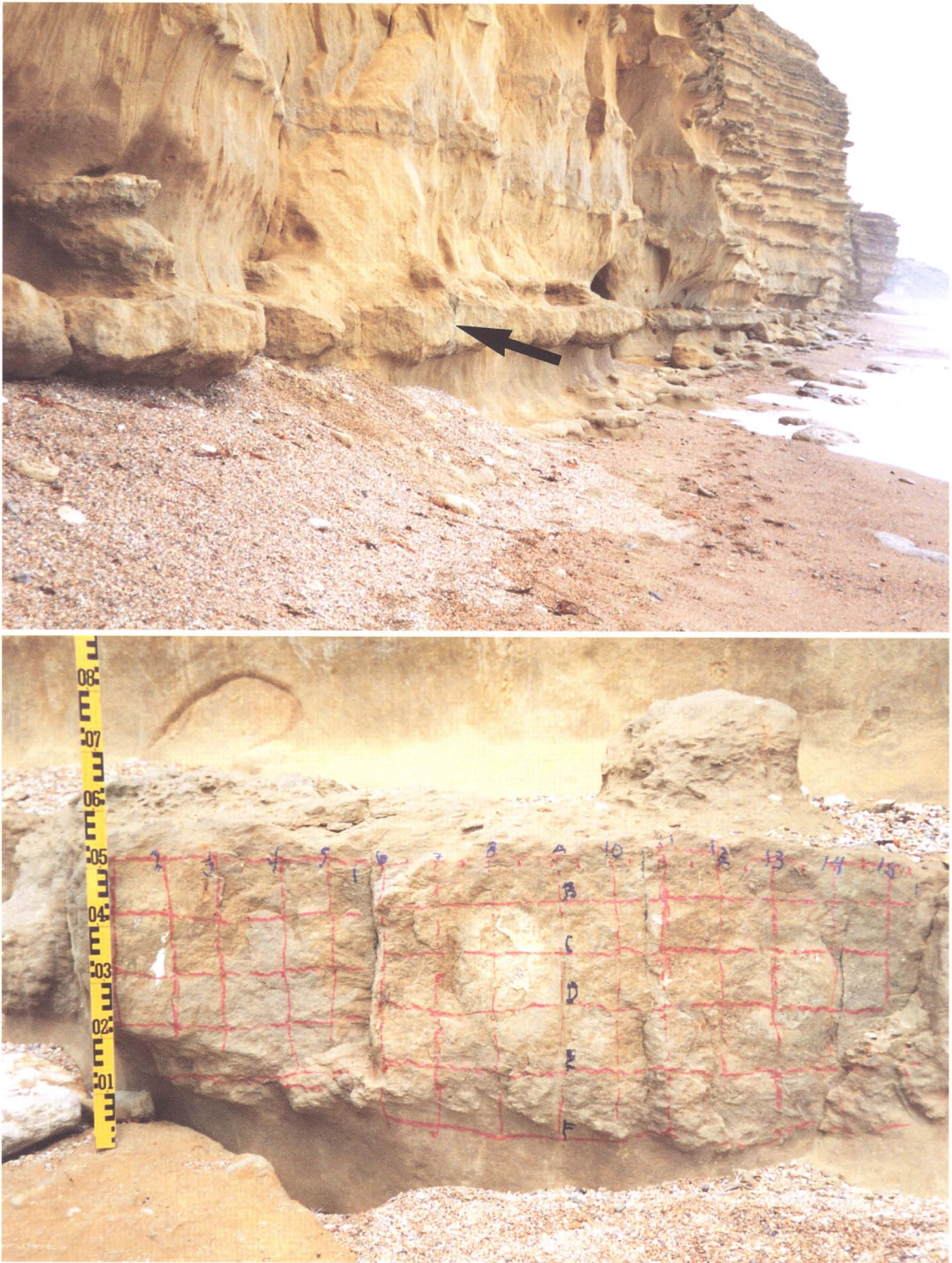
The burial history of the studied exposures of the Bridport Sands is not known with certainty, but the friable nature of the carbonate-cement-free layers and the general lack of quartz overgrowths suggest that burial depth has not exceeded 2–3 km. Porosities of the friable sandstone are 15–37% with a mean of 26% (Davies 1967), which also suggests maximum burial depths of less than 3 km. In the Winterborne Kingston borehole and in the Wyth Farm Oil Field, 40 km and 50 km east of the studied exposures, respectively, the Bridport Sands are now about 1 km below the surface (Knox et al. 1982; Colter and Havard 1981), but present burial depths are up to 2.5 km south of the Purbeck Fault Zone 5 km south of the Wyth Farm Oil Field (Colter and Havard 1981). The Bridport Sands were uplifted in the Tertiary by Alpine compression.

METHODS

Seventy-five of the 107 samples examined were collected from a 10-cm-interval vertical grid 40 cm high and 140 cm long (Fig. 2). In addition, the same calcite-cemented layer, approximately 23 m above the base of the Bridport Sands, was sampled with a 5-cm spacing along three vertical lines located 3.7 m (10 samples), 81.75 m (10 samples) and 82.0 m (12 samples) west of the first 75 samples. Samples approximately 0.1 cm³ in volume were removed with a hammer and chisel. The samples did not show significant alteration due to weathering, although slight differences in color, which correspond to differences in $\delta^{18}\text{O}_{\text{PDB}}$ values of the calcite cement, are apparent. Most of the sampled layer is gray, whereas roughly spherical areas in the central part of the layer are lighter gray to pale brownish white. No open or healed fractures were seen within the sampled grid or at the other sample locations.

Each sample of calcite-cemented sandstone used for isotopic analysis was powdered and heated at 400°C for 4 hr to remove any organic matter. The samples were then reacted with phosphoric acid in vacuum for 2 hr at 25°C, and the CO₂ produced was cleaned through a cold trap (–80°C) before analysis on a Finnigan Mat 251 mass spectrometer. The $\delta^{18}\text{O}$ and $\delta^{13}\text{C}$ values are presented in ‰ relative to the PDB standard. Analytical uncertainty is approximately $\pm 0.1\text{‰}$.

In addition to the samples for isotopic analyses, 11 samples were taken for thin sections. Two samples (A30 and B31) were taken from the calcite-cemented layer, one sample was taken in uncemented sandstone 0.9 m above the calcite-cemented layer, and the last 8 samples were taken from calcite-cemented layers and concretions 1 m, 1.8 m, 2 m, 3 m, and 20 m below the calcite-cemented layer studied. Two thin sections were stained for carbonates with Alizarin Red S and potassium ferricyanide and for K-feldspar with sodium cobalt nitrite, and three thin sections were polished for examination in the cathodoluminescence mode. All thin sections were examined with a standard polarizing microscope and in ultraviolet



(Above) FIG. 1.—Coastal exposure of the Bridport Sands south of Burton Bradstock, Dorset, England. Sampled layer (0.5 m thick) marked by arrow. Cliff is approximately 25 m high.

(Below) FIG. 2.—Close-up view of calcite-cemented layer sampled. Samples were taken at the intersections of the vertical and horizontal lines, i.e., with 10-cm vertical and horizontal spacing. Smallest intervals on scale = 1 cm.

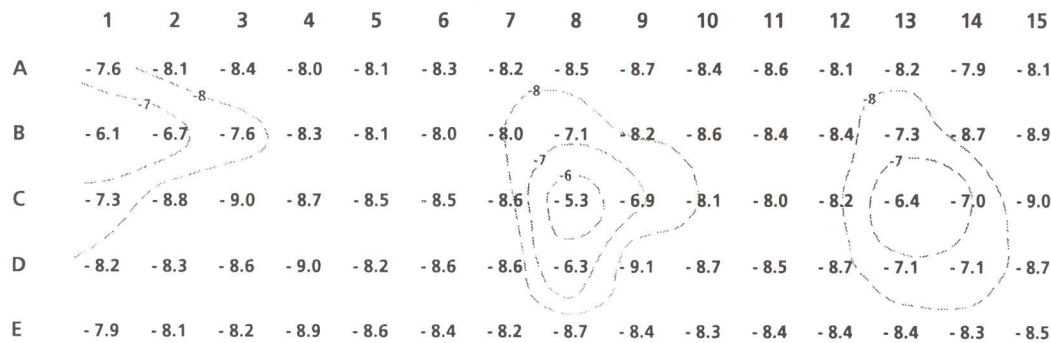


FIG. 3.— $\delta^{18}\text{O}_{\text{PDB}}$ values (in ‰) of calcite cement samples from the grid shown in Figure 2.

and blue light with a fluorescence microscope and point counted with 300 points per thin section. We searched for fluid inclusions in the calcite cement, but none were detected.

PETROGRAPHY

The calcite-cemented samples point counted contain 38–70 volume % siliciclastic material, 26–59% ferroan calcite cement, around 2% carbonate fossil fragments, up to 5% porosity, and minor iron-oxide cement (Table 1). Porosity and iron oxide has probably formed during recent weathering. Quartz is the dominant siliciclastic grain type, accounting for 30–56% of sample volumes; 1–6% K-feldspar is present together with traces of plagioclase, 1–5% muscovite, around 1% biotite, trace amounts of heavy minerals and chlorite, and up to 17% detrital clay. Detrital clay is mostly present as dispersed matrix, and to a lesser degree as clay clasts. Recognizable carbonate fossils include small (< 0.2 mm) fragments of bivalves and/or brachiopods and crinoids; rare phosphatic fossil fragments are also present. Diagenetic components other than calcite cement and recently formed iron oxide are restricted to glauconite within rare pellets plus a few pyrite framboids and pyrite cement specks. Pyrite is engulfed within calcite cement, indicating pyrite precipitation prior to calcite cementation. The observed petrographic composition agrees closely with the petrographic description given previously for the coastal exposures of the Bridport Sands by Davies (1969).

Staining of thin sections, and previously published trace-element data (Walderhaug et al. 1989), show that the calcite cement in the exposures studied is ferroan. Both poikilotopic and finely crystalline calcite is present. Both morphologies may be present within a single calcite-cemented layer, but only poikilotopic calcite was found in the layer analyzed isotopically. Cathodoluminescence and fluorescence microscopy do not reveal any zonation within the calcite cement or more than one generation of calcite cement in any of the samples. The calcite cement is almost nonfluorescent and shows a homogeneous orange cathodoluminescence. Carbonate fossil fragments show approximately the same orange luminescence as the calcite

cement and are often difficult to distinguish from cement. The volume of calcite cement determined by point counting may therefore be too high in some samples. No fractures, open or filled by calcite, were detected in any of the thin sections.

RESULTS OF ISOTOPIC ANALYSES

The $\delta^{18}\text{O}_{\text{PDB}}$ values recorded range from -9.2‰ to -4.8‰ , whereas the $\delta^{13}\text{C}_{\text{PDB}}$ values are confined to the narrow range from -2.2‰ to -0.5‰ . $\delta^{18}\text{O}$ values do not vary randomly within the sampled grid: values less negative than -7.9‰ were found only within three areas in the grid (Fig. 3), and these three areas show a radial decrease in $\delta^{18}\text{O}$ values from -5.3‰ , -6.1‰ , and -6.4‰ at the centers. The three areas with the least negative $\delta^{18}\text{O}$ values correspond to areas with a light gray to pale brownish-white color in the central part of the calcite-cemented layer.

The range of $\delta^{18}\text{O}_{\text{PDB}}$ values recorded along the vertical transects 3.7 m, 81.75 m, and 82.0 m west of the sampled grid is approximately the same as in the two-dimensional grid, i.e., from -4.8‰ to -9.2‰ as compared to -5.3‰ to -9.1‰ for the grid. Two of the vertical profiles show a considerable variation in recorded $\delta^{18}\text{O}$ values, with the least negative values in the central parts of the calcite-cemented layer, and are roughly symmetrical from the middle of the layer and outwards. The third profile shows little variation in $\delta^{18}\text{O}$ values: all measurements fall in the range -8.2‰ to -8.8‰ (Fig. 4). Lighter coloration of the calcite-cemented layer corresponds to $\delta^{18}\text{O}$ values less negative than approximately -8‰ in the vertical transects, as was the case for the analyses in the two-dimensional grid. The results from the vertical profiles are very similar to two previously published vertical isotopic profiles through a calcite-cemented layer in the Bridport Sands (Walderhaug et al. 1989).

DISCUSSION

The $\delta^{18}\text{O}$ data (Fig. 3) may indicate that the calcite cement nucleated at points with lateral spacings on the order of 0.5–1 m within the central

TABLE 1.—Point count results

Sample	Type of Thin Section	Quartz Clasts	K-Feldspar Clasts	Plagioclase Clasts	Muscovite Clasts	Biotite Clasts	Chlorite Clasts	Heavy Minerals	Carbonate Fossils	Phosphatic? Fossils	Glauconitic Clasts	Clay Clasts	Detrital Clay Matrix	Calcite Cement	Pyrite Cement	Iron Oxide Cement	Porosity
W1	polished	56.0	2.3	trace	2.7	0.3	—	0.7	2.3	1.0	trace	0.7	10.3	0.7	trace	1.0	22.0
A30	stained	43.3	5.3	0.3	2.0	trace	—	0.7	1.7	—	trace	1.3	10.3	28.7	—	1.0	5.3
B31	polished	49.3	1.7	trace	1.0	trace	—	0.3	1.3	0.3	trace	1.7	10.3	29.3	—	0.3	4.3
4B	standard	50.0	1.0	trace	5.0	0.7	—	0.3	1.0	trace	trace	1.7	9.0	26.0	trace	3.3	2.0
4A	standard	40.0	1.0	trace	2.7	1.0	—	trace	1.3	trace	trace	2.3	9.3	41.0	—	1.0	0.3
3BT	standard	36.3	1.3	—	2.7	0.3	—	1.0	trace	—	0.3	2.3	14.7	38.0	—	2.3	0.7
3B	standard	38.0	1.3	trace	0.7	0.3	—	0.3	2.0	trace	—	1.0	2.7	52.7	trace	1.0	—
2BT	standard	29.7	2.3	trace	1.0	0.7	—	1.0	2.0	trace	0.3	1.7	1.3	59.3	—	0.7	—
2BM	standard	42.7	1.0	trace	0.7	trace	—	trace	0.3	—	trace	2.3	5.7	46.7	—	0.7	trace
Rip1	stained	35.0	6.3	trace	1.7	0.3	0.3	1.3	2.0	trace	trace	3.0	3.0	44.7	2.0	—	0.3
Rip2	stained	41.7	3.3	trace	2.0	trace	—	trace	1.7	trace	0.3	3.0	7.7	39.0	—	1.3	trace

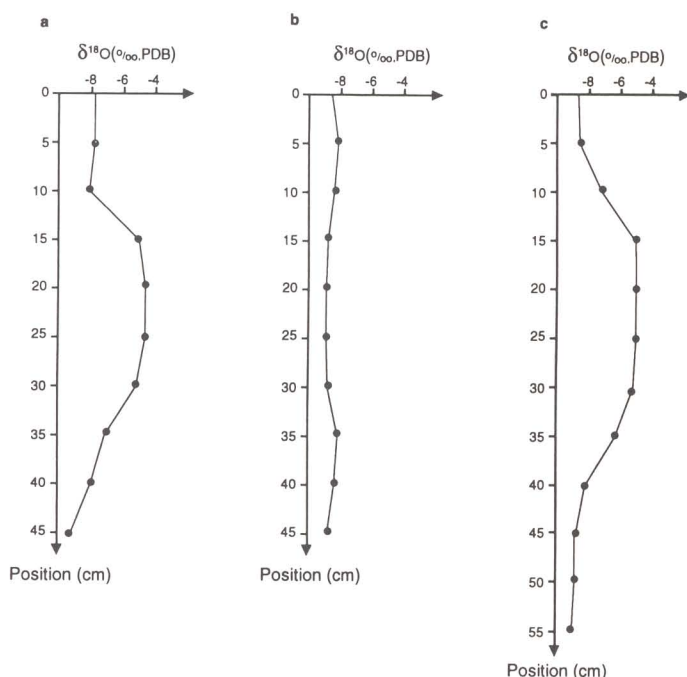


FIG. 4. $\delta^{18}\text{O}_{\text{PDB}}$ values (in ‰) of calcite cement samples taken along vertical lines across the same calcite-cemented layer as in Figures 2 and 3. Sample locations are (a) 82.0 m, (b) 81.75 m, and (c) 3.7 m west of the left-hand (= westernmost) column of the grid in Figure 2.

part of the calcite-cemented layer. The decrease of $\delta^{18}\text{O}$ values outwards from the probable nucleation points suggests further that calcite cement subsequently grew outwards from these nucleation points as individual concretions until the concretions merged to form a continuous layer. Furthermore, the similarity of the $\delta^{18}\text{O}$ values, in both absolute values and trends, at different locations within the calcite-cemented layer (compare Figures 3 and 4) suggests that calcite cementation proceeded contemporaneously and by the same growth mechanism throughout the layer. The $\delta^{13}\text{C}_{\text{PDB}}$ values measured (-2.2‰ to -0.5‰) are close to the $\delta^{13}\text{C}_{\text{PDB}}$ values typical of marine biogenic carbonate (e.g., Hudson 1975), which, together with the presence of carbonate fossil fragments, suggests that biogenic carbonate was the dominant source of the carbon in the calcite cement. Slightly negative $\delta^{13}\text{C}_{\text{PDB}}$ values may, however, also suggest a minor influx of CO_2 from the underlying marine mudstones.

If the calcite cement precipitated from pore water with a $\delta^{18}\text{O}_{\text{PDB}}$ value equal to the probable value for Jurassic sea water, i.e., -1.2‰ (SMOW) (Shackleton and Kennett 1975), then calculated temperatures of precipitation (O'Neil et al. 1969) are in the range $35\text{--}60^\circ\text{C}$. A lighter isotopic composition of the pore water, e.g., more influenced by meteoric water, would give lower temperatures, approximately $20\text{--}40^\circ\text{C}$ for a pore water composition of -4‰ (SMOW). The dominance of $\delta^{18}\text{O}_{\text{PDB}}$ values between -8.0‰ and -9.2‰ suggests that most cementation took place within the higher parts of the suggested temperature ranges.

The suggested interpretation of the radial decrease in the measured $\delta^{18}\text{O}$ values is based on the assumptions that no major shifts in the oxygen isotopic composition of the pore water took place during calcite precipitation and that temperature increased with time during cementation due to increasing depth of burial. The calcite-cemented layer is now exposed at the surface, and the assumption of increasing burial depth, and therefore temperature, as calcite cementation progressed is obviously somewhat uncertain, because calcite cementation may not have been complete before uplift started. Furthermore, data constraining the evolution of the oxygen isotopic composition of the pore water during calcite cementation is lack-

ing. However, even if both significant shifts in isotopic composition of the pore water and uplift with associated temperature decrease took place during precipitation of the calcite cement, the fact still remains that the recorded $\delta^{18}\text{O}$ values decrease symmetrically outwards from points in the middle of the layer. This observation seems very difficult to explain by mechanisms other than radial growth and subsequent merging of concretions, and it is of subordinate importance for the suggested growth mechanism whether the radial variation in $\delta^{18}\text{O}$ values is due to a temperature increase during calcite precipitation, a change in isotopic composition of the pore water during precipitation at a relatively constant temperature, or a combination of these factors.

No open or healed fractures are present within the sample grid, and resetting of isotopic values due to fracturing during uplift and precipitation of calcite cement in the fractures can probably be excluded as a cause of the observed spatial variations in $\delta^{18}\text{O}$ values. It might also be suggested that $\delta^{18}\text{O}$ values could be reset without fractures being present, and that a calcite-cemented layer that for instance originally had approximately the same $\delta^{18}\text{O}$ values throughout would after resetting show a vertical variation in $\delta^{18}\text{O}$ values from the center and outwards, as recorded in two of the vertical profiles (Fig. 4A, C). Such a mechanism would not, however, explain why there is a similar variation in $\delta^{18}\text{O}$ values horizontally (Fig. 3). It is also significant that the coastal exposures of the Bridport Sands contain numerous layers of stratabound calcite-cemented concretions, which according to the model of calcite cementation presented by Bjørkum and Walderhaug (1990) represent layers in which the supply of biogenic carbonate was exhausted before concretions could merge to form a continuous calcite-cemented layer.

CONCLUSIONS

The observed radially symmetrical decrease in $\delta^{18}\text{O}$ values for calcite cement outwards from points in the central parts of the calcite-cemented layer studied suggests that laterally extensive and continuous calcite-cemented layers may form by radial growth and merging of concretions in the manner suggested by Fürsich (1982) and Bjørkum and Walderhaug (1990). Almost identical $\delta^{18}\text{O}$ values and trends in $\delta^{18}\text{O}$ values at different locations within the calcite-cemented layer suggest that cementation took place at the same time and by the same mechanism throughout the layer. Measured $\delta^{13}\text{C}_{\text{PDB}}$ values are close to zero and point to biogenic carbonate as the source for the calcite cement.

ACKNOWLEDGMENTS

Statoil and Esso Norge a.s. are thanked for providing financial support for this study. Rune Mjos is thanked for assistance during sample collection. Isotopic analyses were performed by Ingar Johansen at the Institute of Energy Technology at Kjeller. James R. Boles, Ihsan S. Al-Aasm, and an anonymous reviewer are thanked for constructive reviews.

REFERENCES

- BERNER, R.A., 1980, *Early diagenesis—a theoretical approach*: Princeton, New Jersey, Princeton University Press, 241 p.
- BJØRKUM, P.A., AND WALDERHAUG, O., 1990, Geometrical arrangement of calcite cementation within shallow marine sandstones: *Earth-Science Reviews*, v. 29, p. 145–161.
- BRYANT, I.D., KANTOROWICZ, J.D., AND LOVE, C.F., 1988, The origin and recognition of laterally extensive continuous carbonate-cemented horizons in the Upper Lias Sands of southern England: *Marine and Petroleum Geology*, v. 5, p. 108–133.
- COLEMAN, M.L., AND RAISWELL, R., 1981, Carbon, oxygen and sulphur isotope variations in concretions from the Upper Lias of N.E. England: *Geochimica et Cosmochimica Acta*, v. 45, p. 329–340.
- COLTER, V.S., AND HAVARD, D.J., 1981, The Wyth Farm Oil Field, Dorset, in Illing, L.V., and Hobson, G.D., eds., *Petroleum Geology of the Continental shelf of North-West Europe*: London, Heyden, p. 494–503.
- CONIGLIO, M., AND CAMERON, J.S., 1990, Early diagenesis in a potential oil shale: evidence from calcite concretions in the Upper Devonian Kettle Point Formation, southwestern Ontario: *Bulletin of Canadian Petroleum Geology*, v. 38, p. 64–77.

- DAVIES, D.K., 1967, Origin of friable sandstone-calcareous sandstone rhythms in the Upper Lias of England: *Journal of Sedimentary Petrology*, v. 37, p. 1179-1188.
- DAVIES, D.K., 1969, Shelf sedimentation: an example from the Jurassic of Britain: *Journal of Sedimentary Petrology*, v. 39, p. 1344-1370.
- FÜRSICH, F.T., 1982, Rhythmic bedding and shell bed formation in the Upper Jurassic of east Greenland, in Einsele, G., and Seilacher, A., eds., *Cyclic and Event Stratification*: Berlin, Springer-Verlag, p. 208-222.
- HUDSON, J.D., 1975, Carbon isotopes and limestone cement: *Geology*, v. 3, p. 19-22.
- KANTOROWICZ, J.D., BRYANT, I.D., AND DAWANS, J.M., 1987, Controls on geometry and distribution of carbonate cements in Jurassic sandstones: Bridport Sands, southern England and the Viking Group, Troll Field, Norway, in Marshall, J.D., ed., *Diagenesis of Sedimentary Sequences*: Oxford, Blackwell, p. 103-118.
- KNOX, R.W.O'B., MORTON, A.C., AND LOTT, G.K., 1982, Petrology of the Bridport Sands in the Winterborne Kingston borehole, Dorset, in Rhys, G.H., Lott, G.K., and Calver, M.A., eds., *The Winterborne Kingston borehole, Dorset, England*: Institute of Geological Sciences, Report 81/3, p. 107-121.
- MELVILLE, R.V., AND FRESHNEY, E.C., 1982, *The Hampshire Basin and Adjoining Areas*: Institute of Geological Sciences, London, Her Majesty's Stationery Office.
- MORAD, S., AND ESHETE, M., 1990, Petrology, chemistry and diagenesis of calcite concretions in Silurian shales from central Sweden: *Sedimentary Geology*, v. 66, p. 113-134.
- O'NEIL, J.R., CLAYTON, R.N., AND MAYEDA, T.K., 1969, Oxygen isotope fractionation in divalent metal carbonates: *Journal of Chemistry and Physics*, v. 51, p. 5547-5558.
- SCOTCHMAN, I.C., 1991, The geochemistry of concretions from the Kimmeridge Clay Formation of southern and eastern England: *Sedimentology*, v. 38, p. 79-106.
- SHACKLETON, N.J., AND KENNETT, J.P., 1975, Paleotemperature history of the Cenozoic and the initiation of Antarctic glaciation. Oxygen and carbon isotope analysis in DSDP sites 277, 279, and 281: in Kennett, J.P., Houtz, R.E., et al., eds., *Initial Reports of the Deep Sea Drilling Project*, v. 29, United States Government Printing Office, p. 743-755.
- WALDERHAUG, O., BJØRKUM, P.A., AND NORDGÅRD BOLÅS, H.M., 1989, Correlation of calcite-cemented layers in shallow marine sandstones of the Fensfjord Formation in the Brage Field, in Collinson, J.D., ed., *Correlation in Hydrocarbon Exploration*: London, Graham and Trotman, p. 367-375.
- WILKINSON, M., 1991, The concretions of the Bearreraig Sandstone Formation: geometry and geochemistry: *Sedimentology*, v. 38, p. 899-912.
- WILSON, V., WELCH, F.B.A., ROBBIE, J.A., AND GREEN, G.W., 1958, *Geology of the country around Bridport and Yeoville*: London, Her Majesty's Stationery Office, 239 p.

Received 26 March 1992; accepted 29 January 1993.